Ligand-Specific Conformation Determines Agonist Activation and Antagonist Blockade in Purified Human Thromboxane A2 Receptor†

Ke-He Ruan,* Vanessa Cervantes, and Jiaxin Wu

The Center for Experimental Therapeutics and Pharmacoinformatics, Department of Pharmacological and Pharmaceutical Sciences, College of Pharmacy, 521 Science & Research Building 2, University of Houston, Houston, Texas 77004-5037

Received July 31, 2008; Revised Manuscript Received January 20, 2009

ABSTRACT: The binding of an agonist to a G protein-coupled receptor (GPCR) causes its coupling to different G proteins, which mediate signaling. However, the binding of an antagonist to the same site of the GPCR could not induce coupling. To understand the molecular mechanism involved, the structural flexibility of the purified human thromboxane A_2 receptor (TP) was characterized by spectroscopic approaches, while bound to an agonist or antagonist. Circular dichroism not only revealed that the purified TP adopted more than 50% helical conformation in solution but also showed that the antagonist, SQ29,548, could induce more of a β-sheet structure in the TP than that of the agonist, U46619. Also, fluorescence studies showed that the antagonist induced the intrinsic Trp fluorescence signal change more than the agonist. Furthermore, three of the nine tryptophan residues involved in the different ligand-based structural changes were demonstrated by NMR spectroscopy. Low pH-induced changes in the receptor conformation and molecular interaction field dramatically increased the agonist binding but did not significantly affect the antagonist binding. Different conformational changes were also observed in the TP reconstituted into phosphatidylcholine/phosphatidylserine/phosphatydylethanolamine-formed liposomes. These studies are the first to show a possible mechanism of the ligand-specific conformation-dependent agonist activation and antagonist blockage in the GPCR.

Thromboxane A_2 (TXA_2[1]), which mediates thrombosis and vasoconstriction and plays a key role in the pathological processes of thrombosis, strokes, and heart disease, is also one of the prostanoids synthesized from arachidonic acid through the cyclo-oxygenase pathway (*1, 2*). Like other prostanoids, the biological function of the TXA_2 is mediated by its specific receptor, the TXA_2 receptor (TP), located on the cell membrane. Human TP cDNA was first purified from platelets in 1989 (*3*) and then cloned from placentas in 1991 (*4*), which encode a protein of 343 amino acid residues (*4*). The cDNA for another TP was isolated from human endothelial cells, which have different C-terminal tails, resulting from alternative splicing (*5*), although the signaling properties for the two splice variants are not clearly identified. However, it is known that the endothelium expressed only the spliced form, and the placenta expressed both types of the TP (*5, 6*). Also, like other prostanoid receptors, the TP belongs to the G protein-coupled receptor (GPCR) family and is composed of three intracellular loops and three extracellular loops connecting seven transmembrane (TM) helices. The TP is a promising target for developing antithrombosis and vasoconstriction drugs. However, the lack of a 3D structure for the full length and the presence of an active receptor are major obstacles for further drug development. Recently, through a combination of the NMR spectroscopy technique, site-directed mutagenesis, peptide mimicking, and molecular modeling (*7*−*12*), we have revealed the ligand-recognition site in the extracellular domains and identified that the second extracellular loop (*8, 11, 12*) plays a critical role in forming the ligand-recognition pocket (*8, 10*−*12*). This finding was strongly supported by the recent crystal structure of the β2 adrenergic receptor (a GPCR), in which its second extracellular loop enables ligand access to the binding site (*13*). However, although the 3D structure of the β2 adrenergic receptor has been solved (*13*−*16*), only minimal fundamental information is available to help understand how the ligand activates the native TP signaling in a lipid environment. In addition, the most important structural transition of the TP, where it went from the inactivated ligand-free stage to the activated ligand-bound stage, is particularly interesting in potentially repaving the receptor activation processes.

Here we are reporting a study in which the full length human TP was successfully expressed in Sf-9 cells and efficiently purified to near homogenous levels in a large amount suitable for solution structure characterization using biophysics approaches. The process of activation by its agonist and inhibition by its antagonist, based on the different

* To whom correspondence should be addressed. E-mail: khruan@uh.edu. Tel: 713-743-1771. Fax: 713-743-1884.

† This work was supported by NIH Grants (HL056712 and HL079389 to K.-H.R.).

[1] Abbreviations: TXA_2, thromboxane A_2; TP, TXA_2 receptor; CD, circular dichroism; COSY, correlated spectroscopy; DPC, dodecylphosphocholine; D-M, *n*-dodecyl-β-D-maltoside; PCR, polymerase chain reaction; GPCR, G protein-coupled receptor; PBS, phosphate-buffered saline; PMSF, phenylmethylsulfonyl fluoride; PAGE, polyacrylamide gel electrophoresis; U46619, 9,11-dideoxy-9α,11α-methanoepoxy prostaglandin F2α; NMR, nuclear magnetic resonance; NOE, nuclear Overhauser effect; NOESY, nuclear Overhauser effect correlation spectroscopy; TOCSY, total correlation spectroscopy; 2D, two dimensional; 3D, three dimensional.

10.1021/bi801443g CCC: $40.75
Published on Web 01/26/2009

secondary structure rearrangements of the TP protein, was first revealed by characterization of the purified TP using spectroscopy methods, including fluorescence, CD, and high-resolution NMR spectroscopy.

EXPERIMENTAL PROCEDURES

Materials. D_2O, ethanol-d_6, and DSS (2,2-dimethyl-2-silapentane-5-sulfonic acid) were purchased from Cambridge Isotope Laboratories (Andover, MA). U46619, SQ29,548, and [15-(1α, 2β(5*Z*), 3α-(1*E*, 3*S*), 4α)]-7-[3-hydroxy-4-(*p*-iodophenoxy)-1-butenyl-7-oxabicycloheptenoic acid (I-BOP) were obtained from Cayman Chemicals (Ann Arbor, MI). All other chemicals were purchased from Sigma.

Expression and Purification of the Human TP. Expression and purification of the human TP protein were described previously (*17*). Briefly, a 6His-tag DNA sequence was added to the isolated human TP cDNA at the C-terminal position of the receptor protein to generate the pVL1392-TP-6His construct using a polymerase chain reaction approach. The correct insert and sequence of the TP-6His cDNA were confirmed by restriction enzymes' cutting and DNA sequencing analysis. The pVL1392-TP-6His was packed into baculovirus (BV) with Orbigen Sapphire DNA following the manufacturer's instructions. The recombinant BV was prepared and amplified using Sf-9 cells. The transfected Sf-9 cells expressing the full length and glycosylated TP were evaluated by ligand binding assays, gel electrophoresis staining, and western blot analysis. The TP in the Sf-9 cells was extracted with sodium phosphate buffer (0.01 M, pH 7.2) containing 0.1 M NaCl (in phosphate-buffered saline, PBS), 1% *n*-dodecyl-β-D-maltoside (D-M), 1 mM phenylmethylsulfonyl fluoride, and 40 μg/mL of deoxyribonuclease. The solubilized TP was separated by ultracentrifugation at 250 000*g* for 1 h at 4 °C. The supernatant, rich in TP protein, was purified by a fast protein liquid chromatography system at 4 °C using a Superdex-75 column (1 × 45 cm) with a flow rate of 0.2 mL/min using PBS with 0.1% D-M. The fractions containing the active TP protein were identified by binding assays, polyacrylamide gel electrophoresis (PAGE) analysis, and Western blot.

Electrophoresis and Western Blot. Different amounts of the purified TP (2−10 μg) were separated by 10% PAGE under denaturing conditions and then stained by protein staining or transferred to a nitrocellulose membrane for Western blot, in which a band recognized by an anti-human TP antibody was visualized by a second antibody linked to horseradish peroxidase as previously described (*9*).

Ligand Binding Assay. The ligand binding assay for the TP was performed using a method described by Tai's group (*18*−*20*). The protein sample in 25 mM Tris-HCl buffer, pH 7.4, containing 5 mM $CaCl_2$, was incubated with 3 nM of [^{3}H]-SQ29,548 (30 000 cpm, 30 Ci/mol, Dupont/NEN) in a final reaction volume of 0.1 mL with vigorous shaking at room temperature for 60 min. The reaction was terminated by adding 1 mL of ice-cold washing buffer (25 mM Tris-HCl, pH 7.4). The unbound ligand was filtered through a Whatman GF/B glass filter presoaked in ice-cold washing buffer using a vacuum system. The radioactivity of the TP-bound [^{3}H]-SQ29,548 remaining on the glass filter was counted in 4 mL of scintillation cocktail using a Beckman β Counter. For the competitive inhibition assay, unlabeled SQ29,548 was added.

Fluorescence Spectroscopic Studies for the Interaction of the Purified TP and Its Ligands. The interaction between the purified TP and its ligand was monitored by the fluorescence spectroscopic studies described (*10, 12, 21*). The purified TP was dissolved in 600 μL of sodium phosphate buffer (0.01 M, pH 7.2) containing 0.1 M NaCl and 0.1% D-M. The fluorescence intensity of the tryptophan (Trp) residue(s) in the receptor was monitored fluorometrically at 295 nm for excitation and 335 nm for emission, in the absence or presence of an increasing concentration of the receptor agonist and antagonist on a spectrofluorophotometer (Hitachi, F5000) at room temperature in a 1.0 cm pathlength cell.

Circular Dichroism (CD). CD spectra were recorded with an Olis DSM 1000 CD spectrophotometer, at room temperature, in a 0.1−1.0 cm path-length cell. Each point was taken as the average of four scans. A range of peptide concentrations and solvent conditions were tested.

NMR Spectroscopy Experiments. The purified TP (4 mg) was dissolved in 0.5 mL of 10 mM sodium phosphate buffer, pH 6.0, containing 150 mM NaCl, 10% D_2O, and 0.05% D-M micelles. The 1D ^{1}H spectrum for the receptor was obtained. Later, U46619 (100 μM) was added into the sample (1 mg/50 μL) and incubated at 298 K for 20 min, and the 1D and 2D ^{1}H total correlation spectroscopy (TOCSY) spectra were acquired again. All NMR experiments were carried out on a Bruker Avance 800 MHz NMR spectrometer with a 5 mm triple-resonance probe at 298 K. The water peak was suppressed by the excitation sculpting method (*22*). All 1D spectra contain 16K data points. The nuclear Overhauser effect correlation spectroscopy spectrum was recorded with a mixing time of 150 ms. The TOCSY spectra were carried out with MLEV-17 spin-lock pulse sequence with a total mixing time of 70 ms. Quadrature detection was achieved in the F1 by the states-TPPI method. The NMR spectroscopy data were processed using the Felix 2000 program (Accelrys, San Diego, CA). Shifted sine-bell window functions of 60° for TOCSY were used in both dimensions. Chemical shifts were referenced to the internal standard DSS (contained in the D_2O), which was set to 0 ppm.

Reconstitution of the Purified TP into Lipid Bilayer. The purified TP protein in D-M was reconstituted into a lipid bilayer using phosphatidylcholine/phosphatidylserine/phosphatydylethanolamine (PC/PS/PE) as described previously (*23*).

RESULTS

Secondary Structure of the Active TP in a Lipid Environment Characterized by CD Spectroscopic Analyses. So far, no information has been made available for the secondary structure of the full length human TP in an active form and in a lipid environment. The successful large-scale preparation of the purified TP (*17*) has been the first to provide a sufficient amount of the active receptor protein for CD spectroscopic studies. The purified TP in the mimicked lipid environment with D-M micelles adopts secondary structures with a high helical content as evidenced by a minimum at 220 nm in the CD spectrum (Figure 1). This helix content is

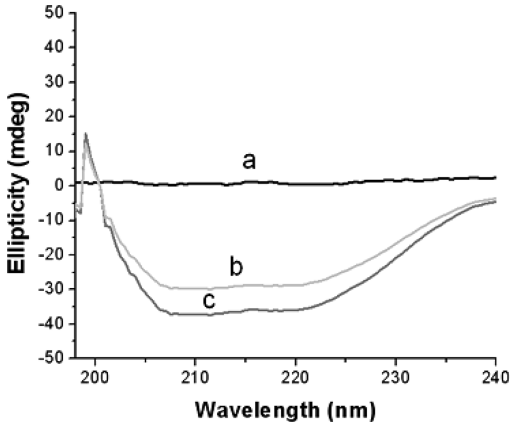

FIGURE 1: Secondary structural analysis for the purified TP protein in a lipid environment using CD spectrometry. The purified TP (0.5 mg/mL, line c) in PBS with 0.1% D-M was measured by an Olis DSM 1000 CD spectrophotometer at room temperature using a 0.1−1 cm path-length cell (0.3 mL). The spectra, which were plotted as the average of four scans, were recorded from 198 to 240 nm. The PBS buffer containing 0.1% D-M detergent (line a) and the positive control, a synthetic peptide (0.5 mg/mL) with an approximately 50% helical structure (line b), are also displayed.

very close to that of the peptide containing approximately 50% of helical conformation as previously determined by CD and 2D NMR spectroscopy (Figure 1, line b) (*24*). Thus, it was predicted that the helical contents of the purified TP protein in the mimicked lipid environment (Figure 1, line c) are very similar to those of the well-defined helical peptide which contains 50% helix in solution (Figure 1, line b). In contrast, the D-M micelles alone did not show any significant absorbance (Figure 1, line a). By analyzing the primary structure of the human TP, it was determined that 45% of the residues in the seven TM domains could adopt a helical structure. The CD results indicated that aside from the 45% of the residues in the TM domains, approximately another 5% of the residues in the receptor's extramembrane domains also adopted helical conformation in this mimicked lipid environment.

Secondary Structure Transition of the Agonist-Activated TP and Its Binding As Characterized by CD Spectroscopic Analysis. How flexible is the secondary structure of the TP upon binding to its ligands? How does the structure information relate to ligand-activated receptor function? These are questions critical for understanding the structure and function relationship of the receptor activation. The purified TP CD spectrum analysis will be very helpful in addressing these fundamental questions. By titrating an increasing amount of the receptor agonist, U46619, to the active receptor in the lipid environment, the secondary structure was significantly perturbed with reduced minimums at 220 nm and increased absorbance at 210 nm (Figure 2) therefore displaying characteristics of slightly decreasing α-helical content. In addition, the corresponding shifts occurred in a saturation manner (Figure 2). These results indicated that the activation of the receptor by the agonist caused a flexible secondary structure change from helix to β-sheet in some segments of the receptor protein, which are likely to have occurred in the extramembrane domains because the TM helix domain is highly constrained.

Secondary Structure Transition of the Antagonist-Inactivated TP and Its Binding As Characterized by CD Spectroscopic Analysis. Little information is known regarding the secondary structure transition for the antagonist inactivation of the TP. A CD experiment was carried out for the purified TP protein where an increasing amount of the antagonist, SQ29,548, was titrated (Figure 3) under conditions identical to those of the agonist. Surprisingly, the secondary structure of the TP protein displayed a different rearrangement with a bigger reduction in helix content and a higher increase in β-sheet content (Figure 3) than that of the agonist activation of the TP shown in Figure 2. The difference was significant and also occurred in a saturation manner. In contrast, Thromboxane B_2, which has no receptor binding activity, did not affect the secondary structure of the purified TP (data not shown). This indicates that the conformational changes induced by the agonist (Figure 2) and antagonist (Figure 3) are specific. These studies strongly suggest that (A) the residues involved in the recognition and binding of the antagonist and agonist are not completely identical and (B) the residues involved in the antagonist interaction have more impact in the secondary structure reconfiguration than that of the agonist. The secondary structure induced by the antagonist, with an increased β-sheet content, could be one of the molecular mechanisms useful in preventing the receptor coupling with the G protein. Furthermore, these results bring about additional interesting inquiries regarding the specific areas of the receptor's extramembrane domains which might be involved in the secondary structure configuration upon interaction with its ligands.

Characterization of the Structural Flexibility of the Purified TP upon Binding to Its Agonist and Antagonist Using Intrinsic Trp Fluorescence Analysis. The intrinsic fluorescent signal of Trp, which is sensitive to local structural change, has been well-characterized (*25*). Previously, conformational changes of the peptide segment mimicking the TP eLP2, upon interaction with the receptor ligand, have been identified by observation of the intrinsic fluorescence intensity of the Trp residues in the eLP2 (*12*). Similarly, the conformational changes of the receptor upon ligand binding that were observed in the CD spectroscopic studies can be further investigated through the observation of changes in the Trp-based intrinsic fluorescence intensity using the purified TP. There are nine Trp residues disturbed in the different protein segments, which include those in the N-terminal domain (Trp2 and Trp29), in the first (Trp95) and second (Trp182) extracellular loops, and those in the TM4 (Trp150 and Trp157), TM6 (Trp258), and TM7 (Trp299 and Trp306). The fluorescence intensity of the intrinsic Trp residues in the purified TP showed an increase following the addition of its agonists, U46619 (Figure 4A, squares), or antagonists, SQ29,548 (Figure 4A, circles), in a concentration-dependent manner, and the residues became saturated with approximately 100 nM of the ligand (Figure 4). Interestingly, the increase in Trp fluorescence intensity induced by the antagonist SQ29,548 was up to 14%, which was almost twice the amount of the agonist, U46619 (7%, Figure 4A). The results suggested that the antagonist induced more structural changes than that of the agonist, which are identical results to those observed in the aforementioned CD studies. This has also clearly revealed that more Trp residues from different segments of the purified TP protein are involved in the structural rearrangement upon the antagonist (SQ29,548) binding rather than agonist (U46619) binding.

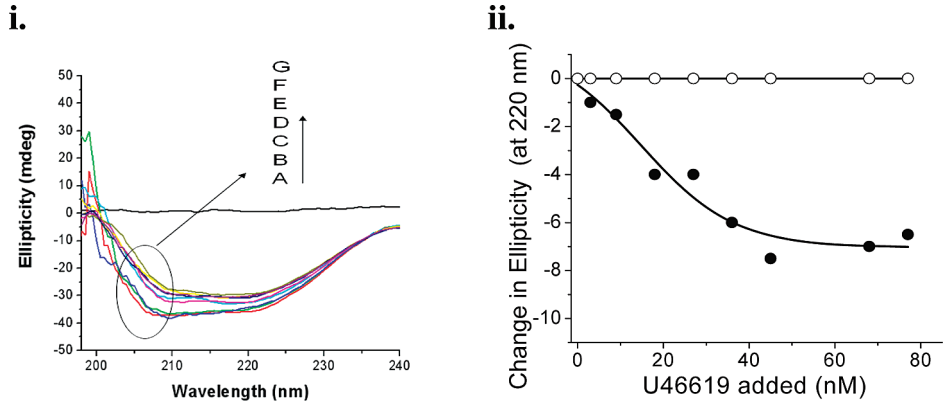

FIGURE 2: (i) Change in the secondary structure of the purified TP in the lipid environment upon binding to its agonist, U46619. The secondary structure of the purified TP was measured by CD spectrometry in the absence (line A) and presence (lines B−G) of an increasing amount of U46619: 1 nM (line B), 3 nM (line C), 10 nM (line D), 30 nM (line E), 60 nM (line F), and 90 nM (line G). The experimental conditions are described in Figure 1. (ii) Dose−response curves showing the change in ellipticity at 220 nm for U46619. Increasing amounts of U46619 were added into the PBS with 0.1% D-M in the presence (closed circles) and absence (open circles) of the purified TP. Each point represents four scans.

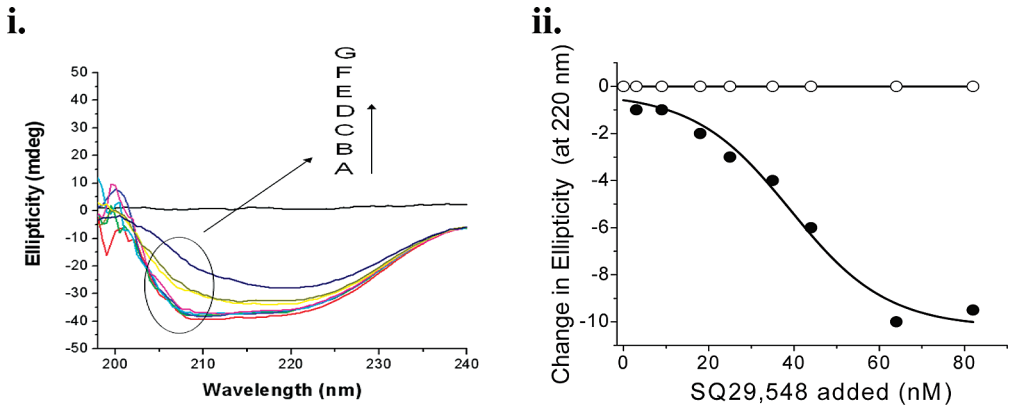

FIGURE 3: (i) Change in the secondary structure of the purified TP in the lipid environment upon binding to its antagonist, SQ29,548. The secondary structure of the purified TP was measured by CD spectrometry in the absence (line A) and presence (lines B−G) of an increasing amount of SQ29,548: 1 nM (line B), 3 nM (line C), 10 nM (line D), 30 nM (line E), 60 nM (line F), and 90 nM (line G). The experimental conditions are described in Figures 1 and 2. (ii) Dose−response curves showing the change in ellipticity at 220 nm for SQ29,548. Increasing amounts of SQ29,548 were added into the PBS with 0.1% D-M in the presence (closed circles) and absence (open circles) of the purified TP. Each point represents four scans.

Competitive Binding of the Agonist and Antagonist with the Purified TP. The Trp-based fluorescence changes were also suitable for identification of the K_d values for the binding of the agonist and antagonist to the TP, which has not thus far been investigated for the purified human TP. From data analysis of Figure 4, the K_d values for U46619 (15 nM) and SQ29,548 (2 nM) were obtained by curve fitting analysis using Origin 6.1 software (OriginLab Corporation, Northampton, MA). The K_d values were very close to that of the previous reported for the human TP (*5*). In addition, another TP agonist, I-BOP with a K_d value of 2 nM (similar to that of SQ29,548), was also measured using the same approach (data not shown). The competitive binding between the agonist and the antagonist for the purified TP protein was further tested by adding increasing amounts of the antagonist, SQ29,548, to the receptor that has been blocked by an excess amount (10 μM) of agonist (I-BOP). Interestingly, the agonist, I-BOP, could only block 80% of the antagonist, SQ29,548, binding (Figure 4B, circles), even though the two ligands have similar K_d values for the receptor. In contrast, the SQ29,548 (10 μM) and I-BOP (10 μM) could completely block the titration of the corresponding antagonist SQ29,548 (Figure 4B, squares) and agonist I-BOP (Figure 4B, triangles), respectively. These results also suggested that the agonist(s) and antagonist share key residues in their binding pockets but are significantly different in other residues which are involved in the configuration of different 2D and 3D binding sites for the ligands as described above. It shall be indicated that the inhibition assay worked for I-BOP and SQ29,548 because they have a similar K_d value; however, U46619, which has much weaker binding than SQ29,548 and I-BOP, is not appropriate for the competition assay.

Characterization of the Structural Flexibility of the Purified TP upon Binding to Its Ligand As Characterized by High-Resolution NMR Spectroscopy. With the successful preparation of the purified TP in the high milligram range, further characterization of the receptor using an NMR spectroscopic technique has become possible. Thus, the structural transition of the purified TP molecule activated by its agonist, as characterized by the CD studies and Trp-based fluorescence method, was further investigated by 2D high-resolution ^{1}H NMR spectroscopy using carefully designed conditions. Although it is difficult to determine the receptor structure using unlabeled protein, the more typical residues, such as Trp, can be easily distinguished since this residue displays a unique chemical shift for its side chain at around 10 ppm without overlapping with other amino acid residues in the protein. This has made it possible for the

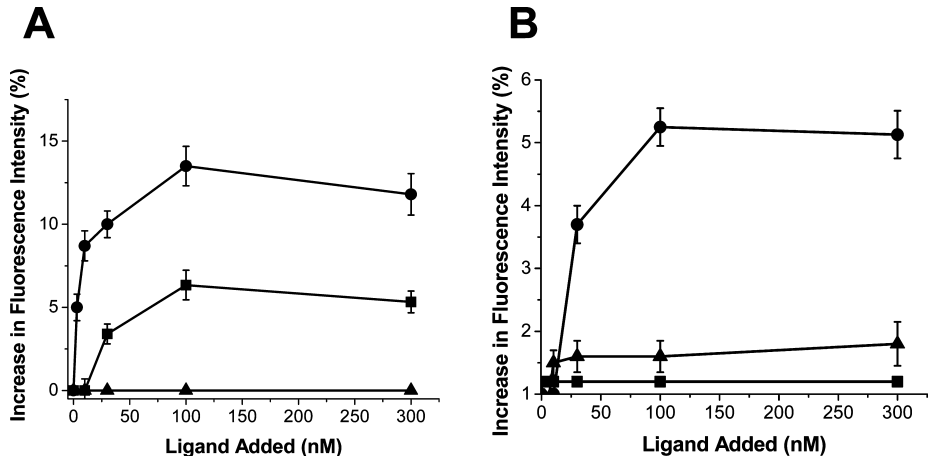

FIGURE 4: (A) Comparison of the conformation changes of the purified TP induced by the ligand using fluorescence spectroscopy. The purified TP (0.05 mg/mL) in PBS containing 0.1% D-M (triangles) was incubated with an increasing amount of its agonist (U46619, squares) or antagonist (SQ29,548, circles), recorded by a fluorescence spectrophotometer using 295 nm for excitation and 335 nm for emission at room temperature, and plotted. (B) Competitive binding of the purified TP with agonist and antagonist. The purified TP (0.05 mg/mL) in PBS containing 0.1% D-M was blocked with 10 μM of I-BOP (circles and triangles) or SQ29,548 (squares) and then incubated with increasing amounts of the ligand [SQ29,548 (circles and squares) or I-BOP (triangles)] from 0 to 300 nM. The increase in the Trp fluorescence intensity was recorded and plotted as described in (A). Fluorescence signals were not observed for the SQ29,548, U46619, or I-BOP alone in the concentration range of 0−300 nM. The results are representative data from three experiments ($n = 3$) and are shown as the mean ± standard error (SE).

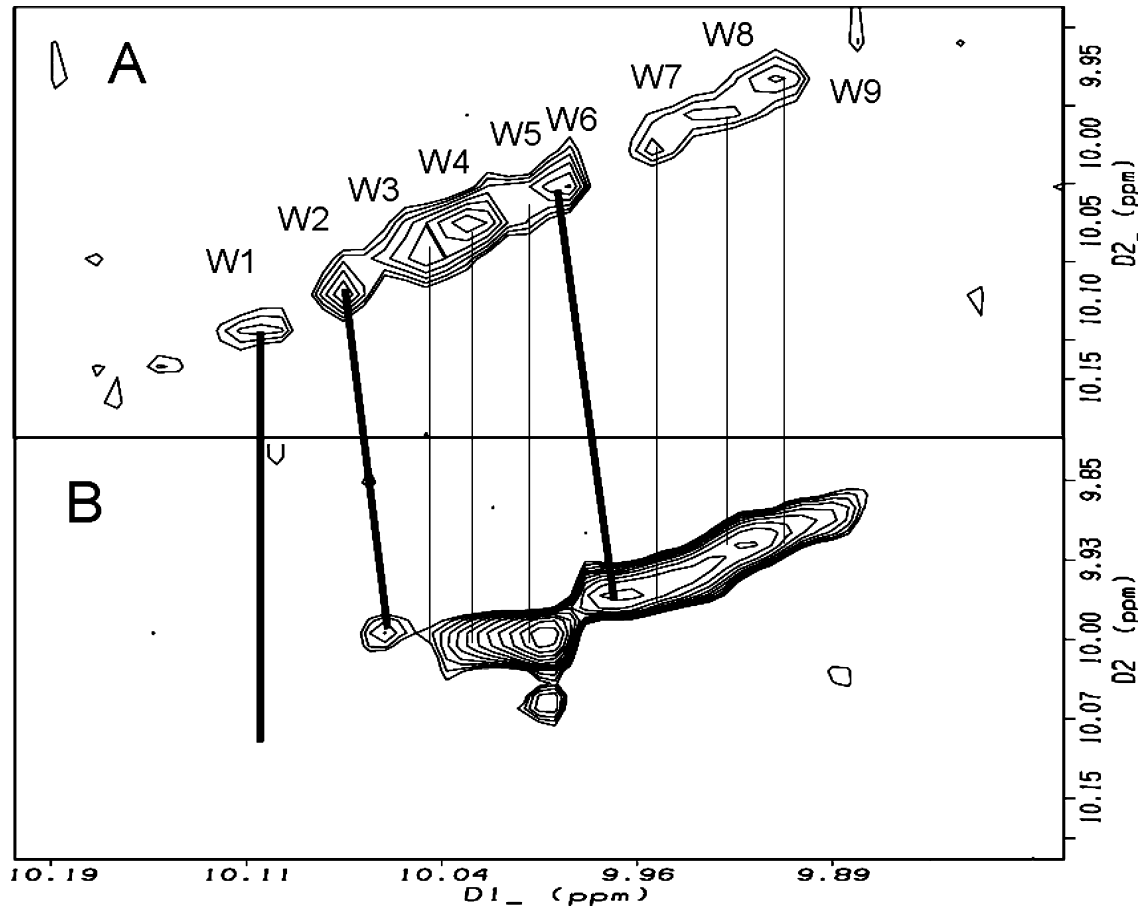

FIGURE 5: Expanded regions of 2D ^{1}H TOCSY spectra for the purified TP bound to its ligands in solution. The spectra for the purified TP were recorded at 298 K on an 800 MHz NMR spectrometer at pH 6.5 as described in Experimental Procedures. The assigned spin systems (between 9.8 and 10.2 ppm) for the indole ring protons of the nine Trp residues from the TP, in the presence of the antagonist, SQ29,548 (A), or the agonist, U46619 (B), with a saturated concentration (100 μM) are shown. The nine Trp residues are labeled from left to right. The cross peaks position changes or complete disappearance (lines with bold) and unchanged cross peaks (lines without bold) between the two spectra are displayed.

purified receptor to be further characterized. It is particularly interesting to determine how many segments containing the Trp residue are involved in the flexible structural change of the receptor when interacting with its ligand. First, the active and purified TP was concentrated and then subjected to high-resolution ^{1}H NMR spectroscopic studies using an 800 MHz

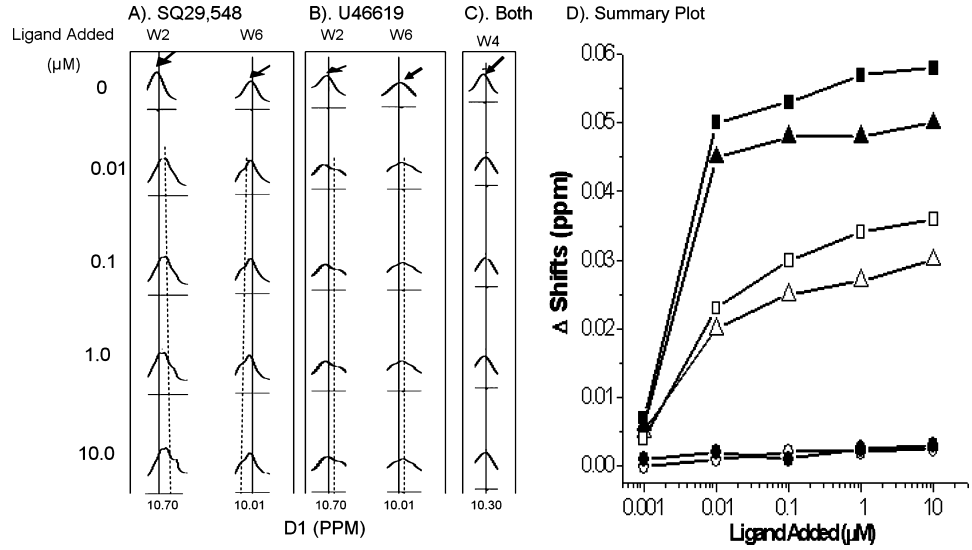

FIGURE 6: Expanded regions for the selected Trp residues in 1D NMR titration experiments. The 1D NMR spectroscopy titration experiments were performed in conditions with fixed protein amounts and increasing amounts of the ligands as indicated in the figures and Experimental Procedures. The positions of the chemical shifts of the corresponding TP Trp residues in the absence (solid lines) and presence (dotted lines) of the ligands are shown (A, B, C). For the chemical shifts of the broadened and split peaks, the peak positions reflecting the averaging between the free and the complexed peaks are used (dotted lines, A and B). The altered ^{1}H chemical shifts (based on the differences between the solid and the dotted lines) of the Trp2 (W2, squares) and -6 (W6, triangles) resulting from the addition of the agonist (U46619, open symbols) or antagonist (SQ29,548, closed symbols) are plotted. The unchanged ^{1}H chemical shift of the Trp4 [W4, shown in panels C and D (circles)] represents the internal control. The purified TP was used for the experiment as described in Figure 5.

instrument. The proton signals belonging to the Trp residues (between 9.9 and 10.2 ppm) in the molecule were observed in the 2D ^{1}H NMR TOCSY spectra for the purified TP bound to SQ29,548 (Figure 5A) or U46619 (Figure 5B). The reason we used TOCSY is because it is relatively sensitive for 2D ^{1}H experiments. The nine Trp residues in the SQ29,548-bound TP were clearly identified in the TOCSY spectrum (Figure 5A). In contrast, the three Trp residues (W1, W2, and W6; Figure 5) in the U46619-bound TP showed different conformations as evidenced by their chemical shift changes. The peak for W1 disappeared, and peaks for W2 and W6 were significantly changed (Figure 5B). This clearly indicated that at least three of the nine Trp residues underwent different conformational changes when the receptor bound to the agonist and antagonist. To further validate the 2D NMR spectroscopic observations, 1D ^{1}H NMR spectroscopy titration experiments were performed for the purified TP in the presence of increasing amounts of the agonist (U46619, Figure 6B) or antagonist (SQ29,548, Figure 6A). The stacked plots show that, in the presence of the receptor ligands, the peaks' response to the W2 and W6 residues of the TP resulted in a broadened second set of peaks, which indicated that the binding of the ligand to the protein was under slow exchange, which agreed with their binding affinity (within the nanomolar ranges) described in Figure 4. In addition, the changes of the chemical shifts (the difference or width between the dotted and the solid lines in Figure 6A,B) for the W2 and W6 that were induced by the antagonist (Figure 6A) were significantly larger than that of the binding with the agonist (Figure 6B). The difference was further summarized using a concentration-dependent plot (Figure 6D). In contrast, the control proton from the TP, W4, was not changed for the ligand titration (Figure 6C). The data further support the conclusion of the 2D NMR spectroscopy experiments (Figure 5), in which the conformational changes of the TP induced by the agonist and the antagonist are different, and the W2 and W6 of the TP are likely to be directly involved in the conformational changes.

Effects of the Low pH-Induced TP Structural Changes on the Agonist and Antagonist Binding. Reducing the neutral pH to an acidic condition can cause protein conformational changes and alteration of the molecular interaction field between ligand and receptor. For example, the lower pH may increase the positive charges for Arg and Lys residues to enhance the electrostatic field and weaken the hydrogen bonds in the ligand binding site of the TP. Low-pH induced conformational changes of the purified TP bound to its ligand, SQ29,548, were first evidenced by the 2D NMR spectrum analysis. Three Trp residues (W1, W7, and W9) of the TP treated with pH 4.5 showed the changes in their chemical shifts in the TOCSY spectrum (Figure 7B) in comparison to that of their conformation in neutral pH conditions (Figure 7A). Surprisingly, the low-pH induced TP conformation and its molecular interaction field increased the agonist, U46619, binding to the receptor (Figure 8A) by 2.5-fold. However, there was no significant change in binding for the antagonist, SQ29,548 (Figure 8B), in the same pH conditions. This further demonstrated that the binding configuration of the agonist to the receptor, which can induce G protein coupling and signaling, is different than that of the antagonist, SQ29,548. It also suggested that the electrostatic field from the positively charged residues in the TP plays an important role in the agonist binding and has little effect on the antagonist binding.

Binding of the Agonist and Antagonist to the Purified TP Reconstituted into Liposomes. To test whether the agonist and antagonist could adopt similar conformational changes for the purified receptor in the phospholipid-mimicked native membrane environment, the purified TP was reconstituted into a liposomal bilayer formed by PC/PS/PE, then interacted with U46619 and SQ29,548, and monitored by fluorescence spectroscopy. As expected, the SQ29,548-induced fluores-

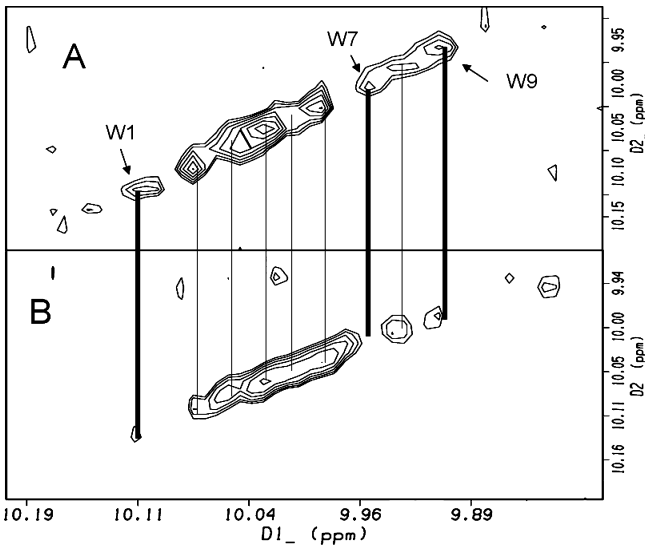

FIGURE 7: Expanded regions of 2D ^{1}H TOCSY spectra for the purified TP bound to SQ29,548 in different pH conditions. The spectra for the purified TP bound to SQ29,548 were recorded at pH 6.5 (A) and pH 4.5 (B) on an 800 MHz NMR spectrometer at 298 K, as described in Experimental Procedures. The assigned spin systems (between 9.8 and 10.2 ppm) for the indole ring protons of the nine Trp residues from the TP are shown. The cross peak changes (lines with bold) and unchanged cross peaks (lines without bold) between the two spectra are displayed.

cence signal change was two-fold higher than that of the U46619 binding (Figure 9), which is identical to that of the receptor incorporated in the D-M micelles (Figure 4A).

DISCUSSION

Even though the crystal structure of the engineered human β2 adrenergic receptor was recently solved, it still remains a challenge to obtain a sufficient amount of other active, full length, and glycosylated human GPCR proteins for structural studies, such as NMR spectroscopy, CD, and crystallization. However, the structural information for human prostanoid receptors, such as TP, are particularly important because these receptors mediate diverse pathophysiological processes and are attractive targets for the next generation of drugs against the top killer diseases, such as hypertension, stroke, and cancers. In this study, the full length and active TP were prepared in large-scale and characterized by the spectroscopic approaches, which led to several interesting new findings: (1) the secondary structure changes of the binding of the agonist and antagonist to the purified TP in the mimicked lipid environment were first identified; (2) the agonist-induced secondary structure, which can couple to the G protein, is different than that of the antagonist bound receptor in solution; (3) the antagonist-bound receptor with a characteristic increase in β-sheet content and decrease in α-helical content indicated that the overall β-sheet structure is an unfavorable conformation for the G protein coupling; and (4) the secondary structure is directly involved in the receptor function upon binding to an agonist and antagonist.

In terms of the binding pocket residues for the full length TP, the studies have strongly suggested that the agonist and antagonist share the ligand-binding pocket in general. Evidence to suggest this can be found in that both ligands induced secondary structure changes with similarly reduced helical content (Figures 2 and 3) and changed the intrinsic

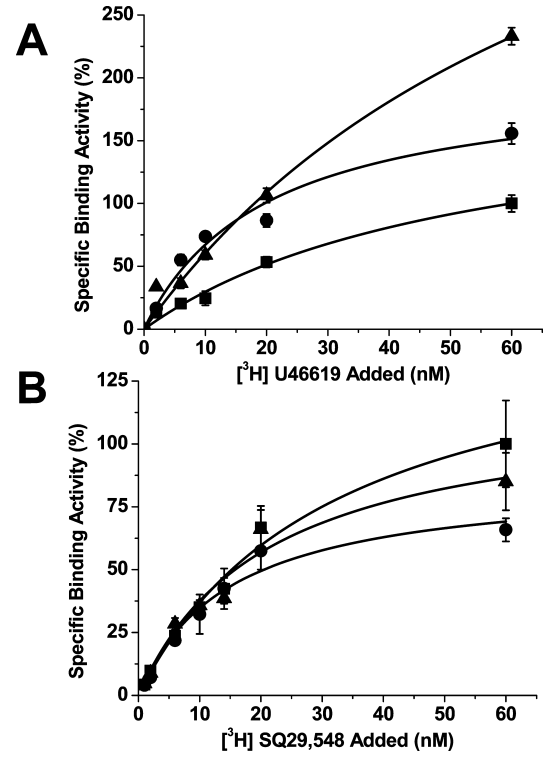

FIGURE 8: Effects of the pH value changes on the agonist and antagonist binding activity for the TP. The bindings of increasing amounts of [^{3}H]-U46619 (A) or [^{3}H]-SQ29,548 (B) to the TP reconstituted into the PC/PS/PE liposomes (10 μg TP protein/tube) at pH 7.0 (squares), 5.5 (circles), and 4.5 (triangles) are plotted. The results are representative data from three assays ($n = 3$) and are shown as the mean ± SE.

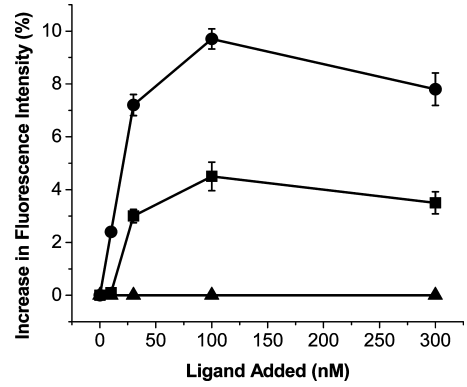

FIGURE 9: Binding of the ligands to the purified TP reconstituted into PC/PS/PE-formed liposomes. The purified TP (0.1 mg/mL) reconstituted into the PC/PS/PE liposomes was incubated with an increasing amount of agonist (U46619, squares), antagonist (SQ29,548, circles), or PBS (triangles) and then recorded by a fluorescence spectrophotometer as described in Figure 4A. The results are representative data from two assays ($n = 2$) and are shown as the mean ± SE.

Trp fluorescence intensity. In addition, the agonist blocked 80% of the antagonist binding (Figure 4B, squares). However, the studies also suggested that the configuration of the binding pocket for the agonist, U46619, and antagonist, SQ29,548, are quite different since the antagonist induced more of a β-sheet structure than that of the agonist and also because the additional agonist, I-BOP, could not completely block the antagonist, SQ29,548, binding to the TP and induce the conformational change (Figure 4B). So far, there is a very limited amount of information regarding the structure

and function relationship for the full length TP that could help explain the unique agonist and antagonist binding in structural terms. These studies have revealed a possible molecular mechanism of the agonist and antagonist actions on the receptor, in which the TP receptor signaling is turned on by the correct secondary and 3D conformation, induced by the agonist, and turned off by the incorrect (unfavorable β-sheet content in the extramembrane domains) secondary and 3D conformation induced by the antagonist. This mechanism might be suitable for other prostanoid receptors or other GPCRs.

Agonist-induced intrinsic Trp fluorescence change of the purified TP caused by the receptor activation has been evidenced in the studies. It has become very interesting to determine how many Trp residues actually participated in the conformational change when the receptor was activated by its agonist, U46619. The NMR spectroscopic technique is a useful technique for addressing this question when purified TP protein is available. Three of the nine Trp resides underwent conformational changes as shown in the TOCSY spectrum (Figure 5), which has provided evidence to suggest that at least the segments containing the three Trp residues in the TP are involved in the conformational alteration upon the agonist activation. We expect that at least two Trp residues within the first and second extracellular loops are very likely to be involved in the ligand-induced conformation change. This speculation is supported by the following reasons: (1) Previously, we reported that ligands could increase the fluorescence intensity of the Trp residue in the eLP2 segment of the human TP (*8*). Thus, one of the two Trp residues' response to the TP protein conformational change is likely in the eLP2. (2) Another Trp residue is in the eLP1 which is linked to the eLP2 by a disulfide bond through Cys102 in the eLP1 and Cys183 in eLP2. The ligand-induced conformation change in the eLP2 will affect that of the eLP1 conformation. The antagonist (SQ29,548)-induced increase in the intrinsic Trp fluorescence intensity (14%) was twice the amount of the agonist U46619 (7%, Figure 4A). Thus, there should not be any difficulty in predicting that there are more Trp residues involved in the antagonist-induced conformational change on the TP than in that of the agonist (U46619)-induced. There are two Trp residues in TM7, which are involved in forming the antagonist binding site. Therefore we could not exclude the possibility that alternating Trp residues' conformation in the TM7 by the antagonist may be involved in the blockage of the receptor signaling.

There was a significant increase in agonist, U46619, binding to the TP in acidic conditions (Figure 8A). However, an increase in binding was not observed during the antagonist, SQ29,548, binding to the receptor. This raises the possibility that the configuration of the agonist and antagonist (in binding to the receptor) are significantly different. This could be the result of different conformations of the TP or different protonation stages of the ligands in the acidic conditions. This remains to be further characterized.

One of the most interesting findings in these studies is that the low-pH induced conformation and the molecular interaction field for the purified TP were able to distinguish the binding characteristics for the agonist (increasing binding capacity) and antagonist (no significant change) in the mimicked lipid environment (Figure 8). It provided strong evidence indicating that the residues in the TP, such as Arg and Lys, are likely involved in the agonist binding-induced TP−G protein coupling but are not important to the antagonist binding, which blocked the TP−G protein interaction. The study also implies that such characteristics could be present in other prostanoid receptors because of the similarities among the ligands and protein sequences.

Finally, it should be indicated that the chemical shift changes in the NMR titration for the interaction between the TP and the ligands could also be seen if the aromatic groups on the agonist or antagonists were physically proximal to Trp side chains of the TP protein. Thus, our conformational change is a broadened term in this study, which consists of a situation where the side chains of the ligand are close to the Trp residues. As a conclusion, all of the findings support a hypothesis, which suggests that the ligand (agonist or antagonist)-induced specific receptor conformation is one of the possible molecular mechanisms involved in agonist activation and antagonist blockage for the TP signaling. This hypothesis might also be applied to other prostanoid receptors in general.

ACKNOWLEDGMENT

We thank Dr. Xiaolian Gao in the Chemistry Department and Dr. Youlin Xia in the KECK/IMD NMR Center of the University of Houston, for access to the NMR facility and for providing valuable advice on taking the NMR spectra. The acknowledgement is also made to Dr. Glen Legge in the Biochemistry Department, University of Houston, for access to the CD spectrophotometer and his assistance as well.

REFERENCES

1. Majerus, P. W. (1983) Arachidonate metabolism in vascular disorders. *J. Clin. Invest. 72*, 1521–1525.
2. Samuelson, B., Goldyne, M., Granstrom, E., Hamberg, M., Hammarstrom, S., and Malmsten, C. (1978) Prostaglandins and thromboxanes. *Annu. Rev. Biochem. 47*, 994–1030.
3. Ushikubi, F., Nakajima, M., Hirata, M., Okuma, M., Fujiwara, M., and Narumiya, S. (1989) Purification of the thromboxane A2/prostaglandin H2 receptor from human blood platelets. *J. Biol. Chem. 264*, 16496–16501.
4. Hirata, M., Hayashi, Y., Ushikubi, F., Yokata, Y., Kageyama, R., Nakanishi, S., and Narumiya, S. (1991) Cloning and expression of cDNA for a human thromboxane A_2 receptor. *Nature 349*, 617–620.
5. Raychowdhury, M. K., Yukawa, M., Collins, L. J., McGrail, S. H., Kent, K. C., and Ware, J. A. (1994) Alternative splicing produces a divergent cytoplasmic tail in the human endothelial thromboxane A2 receptor. *J. Biol. Chem. 269*, 19256–19261.
6. Hirata, T., Ushikubi, F., Kakizuka, A., Okuma, M., and Narumiya, S. (1996) Opposite coupling to adenylyl cyclase with different sensitivity to Arg60 to Leu mutation. *J. Clin. Invest. 97*, 949–956.
7. Wu, J., Feng, M., and Ruan, K. H. (2007) Assembling NMR structures for the intracellular loops of the human thromboxane A(2) receptor: Implication of the G protein-coupling pocket. *Arch. Biochem. Biophys. 470*, 73–82.
8. Ruan, K. H., Wu, J., So, S. P., Jenkins, L. A., and Ruan, C. H. (2004) NMR structure of the thromboxane A2 receptor ligand recognition pocket. *Eur. J. Biochem. 271*, 3006–3016.
9. Geng, L., Wu, J., So, S. P., Huang, G., and Ruan, K. H. (2004) Structural and functional characterization of the first intracellular loop of human thromboxane A2 receptor. *Arch. Biochem. Biophys. 423*, 253–265.
10. Wu, J., So, S. P., and Ruan, K. H. (2003) Solution structure of the third extracellular loop of human thromboxane A2 receptor. *Arch. Biochem. Biophys. 414*, 287–293.
11. So, S. P., Wu, J., Huang, G., Huang, A., Li, D., and Ruan, K. H. (2003) Identification of residues important for ligand binding of thromboxane A2 receptor in the second extracellular loop using

the NMR experiment-guided mutagenesis approach. *J. Biol. Chem. 278*, 10922–10927.
12. Ruan, K. H., So, S. P., Wu, J., Li, D., Huang, A., and Kung, J. (2001) Solution structure of the second extracellular loop of human thromboxane A2 receptor. *Biochemistry 40*, 275–280.
13. Cherezov, V., Rosenbaum, D. M., Hanson, M. A., Rasmussen, S. G., Thian, F. S., Kobilka, T. S., Choi, H. J., Kuhn, P., Weis, W. I., Kobilka, B. K., and Stevens, R. C. (2007) High-resolution crystal structure of an engineered human beta 2-adrenergic G protein-coupled receptor. *Science 318*, 1258–1265.
14. Ranganathan, R. (2007) Biochemistry. Signaling across the cell membrane. *Science 318*, 1253–1254.
15. Rosenbaum, D. M., Cherezov, V., Hanson, M. A., Rasmussen, S. G., Thian, F. S., Kobilka, T. S., Choi, H. J., Yao, X. J., Weis, W. I., Stevens, R. C., and Kobilka, B. K. (2007) GPCR engineering yields high-resolution structural insights into beta 2-adrenergic receptor function. *Science 318*, 1266–1273.
16. Rasmussen, S. G., Choi, H. J., Rosenbaum, D. M., Kobilka, T. S., Thian, F. S., Edwards, P. C., Burghammer, M., Ratnala, V. R., Sanishvili, R., Fischetti, R. F., Schertler, G. F., Weis, W. I., and Kobilka, B. K. (2007) Crystal structure of the human beta 2 adrenergic G-protein-coupled receptor. *Nature 450*, 383–387.
17. Ruan, K. H., Cervantes, V., and Wu, J. (2008) A simple, quick, and high yield preparation of the human thromboxane A2 receptor in full size for structural studies. *Biochemistry 47*, 6819–6826.
18. Chiang, N., and Tai, H. H. (1998) The role of N-Glycosylation of human thromboxane A2 receptor in ligand binding. *Arch. Biochem. Biophys. 352*, 207–213.
19. Chiang, N., Kan, W. M., and Tai, H. H. (1996) Site-directed mutagenesis of cysteinyl and serine residues of human thromboxane A2 receptor in insect cells. *Arch. Biochem. Biophys. 334*, 9–17.
20. Zhou, H., Yan, F., and Tai, H. H. (2001) Phosphorylation and desensitization of the human thromboxane receptor-alpha by G protein-coupled receptor. *J. Pharmacol. Exp. Ther. 298*, 1243–1251.
21. Zhang, L., Huang, G., Wu, J., and Ruan, K. H. (2005) A profile of the residues in the first intracellular loop critical for Gs-mediated signaling of human prostacyclin receptor characterized by an integrative approach of NMR-experiment and mutagenesis. *Biochemistry 44*, 11389–11401.
22. Lin, Y., Wu, K. K., and Ruan, K.-H. (1998) Characterization of the secondary structure and membrane interaction of the putative membrane anchor domain of prostaglandin I2 synthase and cytochrome P450 2C1. *Arch. Biochem. Biophys. 352*, 78–84.
23. Callihan, D., West, J., Kumar, S., Schweitzer, B. I., and Logan, T. M. (1996) Simple, distortion-free homonuclear spectra of peptides and nucleic acids in water using excitation sculpting. *J. Magn. Reson., Ser. B 112*, 82–85.
24. Ruan, K. H., So, S. P., Zheng, W., Wu, J., Li, D., and Kung, J. (2002) Solution structure and topology in membrane-bound prostacyclin synthase. *Biochem. J. 368*, 721–728.
25. Dahms, T. E., and Szabo, A. G. (1995) Probing local secondary structure by fluorescence: time-resolved and circular dichroism studies of highly purified neurotoxins. *Biophys. J. 69*, 569–576.

BI801443G